Technoscience Journal for Community Development in Africa 5:1 (2026) 71–81
ISSN 2659-0573

Research Article

Screening of repurposable natural products database to identify potent small-molecule inhibitors of SARS-CoV-2 spike glycoprotein

Yusuf Oloruntoyin Ayipo[1,2], Yahaya Sani Najib[1,3], Waleed A. Alananzeh[1], Zainab Funmi Adebayo[2], Mohd Nizam Mordi[1]

[1]Centre for Drug Research, Universiti Sains Malaysia, USM, 11800, Pulau Pinang, Malaysia
[2]Department of Chemistry and Industrial Chemistry, Kwara State University, P. M. B., 1530, Malete, Ilorin, Nigeria
[3]Department of Pharmaceutical and Medicinal Chemistry, Bayero University, Kano, Nigeria

Abstract: Interaction between the RNA binding domain (RBD) of the SARS-CoV-2 spike glycoprotein (S-protein) and human angiotensin-converting enzyme 2 (ACE2) has been implicated in the viral entry into host cells. S-protein has become an essential constituent of the currently approved vaccines. S-protein may be inhibited by antibodies and peptides, but the inhibitions are usually characterised by instability and membrane impermeability. Hence, it is imperative to search for stable inhibitors. In this study, 2826 FDA-approved natural small-molecule drugs were screened against the pre-fusion SARS-CoV-2 S-protein (PDB 6VSB) using molecular docking and molecular dynamics simulations. Notably, lonafarnib, (-)-epicatechin gallate, melibiose, lactitol monohydrate and maltitol, showed strong binding interactions with the RBD of S-protein, with extra precision (XP) docking scores of -12.17, -11.67, -11.66, -11.30 and -10.74 kcal/mol respectively. It was referenced against remdesivir and ribavirin with XP docking scores of -9.10 and -6.05 kcal/mol respectively. Consistently, their respective molecular mechanics generalized Born surface area continuum solvation MMGB(SA) binding free energies, -18.48, -48.13, -30.01, -37.27 and -15.31 kcal/mol support their higher inhibitory potentials compared to the two references. They interacted with active site residues that are pharmacologically essential for blocking the S-protein-ACE2 that is responsible for SARS-CoV-2 infectivity, and displayed thermodynamic stability. The drugs showed promising potential as repurposable anti-SARS-CoV-2 candidates and therefore recommended for clinical studies

Keywords: SARS-CoV-2, S-glycoprotein, ACE2, Molecular interactions, Drug repurposing

1. Introduction

The coronavirus disease 2019 (COVID-19) pandemic as termed by the WHO (Zhang et al., 2020) continues to threaten the global healthcare system, economy and population through daily infections and loss of lives. Hence, it is declared as public health emergency of international concern (PHEIC) (Atri et al., 2020; Zhang et al., 2020). Since its outbreak in 2019, COVID-19 has been reported to claim 4,890,002 lives, representing 2.04% of the 239,973,258 people infected globally while 217,312,227 patients have recovered, as of October 14, 2021 (Woldometer.info, 2021). The main pathology remains under study (Zhang et al., 2020). However, according to virologists, severe acute respiratory syndrome coronavirus 2 (SARS-CoV-2) is a β-CoV family member of coronaviridae of the order Nidovrales. Similarly to SARS-CoV-1 and the Middle East respiratocy syndrome (MERS)-CoV, it is characterised by an enveloped single-stranded positive ribonucleic acid (RNA) and a crown-like density of proteinous membrane (corona) for binding to targets (Atri et al., 2020; Ayipo et al., 2021). Upon gaining entrance into the host respiratory tract, the SARS-CoV-2 binds to host cells via the membrane-bound angiotensin-converting enzyme 2 (ACE2), which is preceded by the use of androgen-responsive transmembrane protease serine 2 (TMPRSS2) for spike (S) protein priming.

* Corresponding author:
Email: yusuf.ayipo@kwasu.edu.ng

KWASU PRESS AND PUBLISHING

The progression of the process results in the viral RNA fusion and subsequently replication. These strongly implicate the viral S protein and human ACE2 interplay in the viral infectivity and as a plausible therapeutic target (Atri et al., 2020; Ayipo et al., 2021; Hoffmann et al., 2020).

Thus, inhibitory effects against the signal pathway of viral S-protein and the blockade of human host cell protease, ACE2, constitute a therapeutic strategy to prevent SARS-CoV-2 entry into cells. In addition to the viral periodic genetic mutations, the difficulty in understanding the main aetiology contributes to the scarcity of effective anti-SARS-CoV-2 inhibitors of human ACE2 till moment (Wu et al., 2020). The human ACE2 is reportedly inhibited mostly by antibodies and peptides which are usually characterised by in vivo instability, membrane impermeability, less controllable and immunogenic (Bojadzic et al., 2021; Lee et al., 2019; Zhou et al., 2021). Some of these drawbacks could be mediated by small-molecule drugs, as parts of the mega trials recommended by the World Health Organisation for COVID-19 (Bojadzic et al., 2021). However, only few inhibitors of this type have been reported, none of which had successfully passed clinical studies. These include nelfinavir mesylate, a protease inhibitor of human immunodeficiency virus which suggestively binds to the S trimer structure to prevent S-n and S-o-mediated cell fusion (Musarrat et al., 2020). Others are amantadine and teicoplanin which reportedly supress the catalytic activity of cathepsin L, and ribavirin and tenofovir from a recent computational study (Unni et al., 2020; Xiang et al., 2021). These results suggests robust anti-SARS-CoV-2 inhibitors may be found from a wider search among small molecules. And applications of relationship between genomic information and pathological features of the viral infectivity can aids identification of prospect small molecule candidates (Kupferschmidt & Cohen, 2020; Wu et al., 2020). Search for prospect small molecule candidates from existing FDA-approved natural products drugs is attractive because it can be carried out in a record time. This strategy is particularly cost-effective since FDA-approved natural products drugs have established pharmacokinetics, pharmacodynamics and toxicological profiles for immediate trial.

Computational and bioinformatics methods had been deployed to study cellular factors of SARS-CoV-2 isolate, to predict its mode of infection and to gain insights about effective therapeutic strategies for drug development (Robson, 2020). Molecular docking and molecular dynamic (MD) can be mimic biomolecular interactions outside cellular environments, thus, they are screening tools in drug development efforts. Although some small molecules such as remdesivir, ribavirin, sofosbuvir and theaflavin(Elfiky, 2020; Lung et al., 2020; Wu et al., 2020), had been suggested as potent inhibitors against COVID-19, in this study, we use molecular docking and MD simulations to screen small molecules from a larger pool. We screen the molecules in the repurposing library of Selleckchem.com Bioactive compounds expert (https://www.selleckchem.com/screening/drug-repurposing-library.html), in the quest to identify potent inhibitors of the SARS-CoV-2 S-glycoprotein entry through human ACE2. The theoretical inhibitory potentials, thermodynamic stability and biological applicability, of the most promising candidates from our search were compared with those of remdesivir and ribavirin (Jin et al., 2020; Lung et al., 2020; Ton et al., 2020; Wu et al., 2020)..

2. Materials and methods

2.1. Ligand preparation

The structure data file (SDF) of the reference inhibitors (remdesivir and ribavirin) were downloaded from the Pubchem database. SDF of 2826 natural product drug molecules were downloaded from the Selleckchem.com drug repurposing library (Kim et al., 2021). The files were imported into the Maestro 12.12 workspace for preparation using LigPrep (LigPrep, Schrodinger, LCC, New York, NY, 2019). The protocols involved Epik target energy minimization at pH 7.0 ± 2.0, addition of hydrogens and conversion of 2D to 3D structures. The geometry and partial atomic charges were estimated using the OPLS-3e force field (Schrodinger, 2019-Version LigPrep) while the prepared protonated ligand conformers were saved in the LigPrep output file.

2.2. Analysis of receptor active cavity

The crystal structures of the receptors, the viral pre-fusion S-protein, was retrieved from the RCSB protein data bank (PDB) with the identity PDB 6VSB. Its active ligand-binding pockets were analysed in line with literature reports (Lan et al., 2020; Padilla-Sanchez, 2020; Unni et al., 2020) and RESIDUE-DEPTH server. The PDB file was uploaded to the server for the depth predictions in terms of the probability of amino acid residue forming binding sites, the dissociation constant (pKa) and the binding cavity coordinates at a default solvent neighbourhood radius of 4.2Å, probability threshold 0.8 and the minimum number of neighbourhood-solvent maintained at default settings

(Choudhary et al., 2020; Tan et al., 2013; Yu et al., 2020).

2.3. Protein preparation and receptor grid generation

The PDB file of the crystal structures of the selected receptor was prepared through pre-processing, optimization by assigning protonation states and partial atomic charges, followed by refinement through deletion of water and other covalently linked molecules, and moderation of bond order. Energy minimization was configured by using optimized potentials for liquid simulations 3e (OPLS-3e) force field incorporated in Maestro 12.2 (Schrodinger, 2019-Version Protein Preparation Wizard) and the convergence of heavy atoms to a root mean square deviation (RMSD) of 0.3 Å. Then the removal of non-focused chains was followed by the assignment of x, y, z coordinates to generate ligand-docking grid box.

2.4. Molecular docking simulations

Molecular docking was carried out to evaluate the inhibitory potentials of each minimized drug conformer against the receptor through interactions with the amino acid residues in its pocket using Maestro 12.2 Glide high throughput virtual screening, then XP docking module (Schrodinger, 2019-Version) (Halgren et al., 2004). The results were ranked in ascending order of XP glide scores while the bonded and non-bonded interactions were analysed using the generated 2D binding poses in comparison to the reference control inhibitors.

2.5. Molecular dynamics

Ligand-receptor complexes that gave cumulative high XP gscores and good binding poses were selected for MD simulations. The MD simulations will help evaluate stability of the ligand-receptor complexes in comparison with reference drugs, remdesivir and ribavirin, which are currently in the clinical trials of COVID-19. The binding affinity, conformational and thermodynamic stability, and flexibility trajectories of the selected ligands in complex with the receptor were studied using molecular mechanics (MM) force field available in Ligand and Receptor MD (LARMD) server integrated with AMBER 16 force field (http://agroda.gzu.edu.cn:9999/ccb/server/LARMD/) (Yang et al., 2019). Each of the selected ligand-receptor complexes was uploaded for 'Int-mod' simulation, setting the all-atom MD time at 3000 ps, solvation model and other parameters were set adopting relevant protocols (Yang et al., 2019; Kumar et al., 2020; Fatoki et al., 2021; Pervez et al., 2020). The 3000 ps timeframe set for the MD simulation is in accordance with the limitation of 4000 ps accepted to be run on the server (Yang et al., 2019). Moreover, several similar studies have conducted MD simulations successfully for analysisng the stability ligand-receptor complex involving SAR-CoV-2 targets within a timeframe of 1000-4000 ps using the same server (Kumar et al., 2020; Fatoki et al., 2021; Pervez et al., 2020). The RMSD plot was generated to study the deviation in the average distances between the atoms of the docked ligands from their original positions while the RMS distance between each protein atom to their control was represented by the radius of gyration (rGyr) plot. The conformational dynamics of each ligand-receptor complex system and energetics of the selected binding ligands, explored by capturing the transition states of the receptor with a folding free energy barrier is presented as the fractions of native contacts. The isotropic fluctuations and displacements, occuring on each amino acid along the trajectory of simulation, indicating the drug-protein stabilities were depicted by the B-factor and RMS fluctuation (RMSF) plot. The molecular mechanics generalized Born surface area continuum solvation, MMGB(SA) re-scoring methods and the plots of statistics of hydrogen bonds were employed for theoretical estimation of the binding affinities and binding free energies, represented by ΔGbind as shown in equation (i-iv) (Ayipo et al., 2021; Karplus & Petsko, 1990; Kesheri & Sinha, 2016).

$$\Delta G_{bind} = G_{complex} - G_{receptor} - G_{ligand} \quad \text{(i)}$$

$$= \Delta H - T\Delta S \approx \Delta E_{gas} + \Delta G_{sol} + T\Delta S \quad \text{(ii)}$$

$$\Delta E_{gas} = \Delta E_{int} + \Delta E_{ele} + \Delta E_{vdw} \quad \text{(iii)}$$

$$\Delta G_{sol} = \Delta G_{GB} + \Delta G_{surf} \quad \text{(iv)}$$

Where ΔH is the enthalpy change, ΔEgas for gas-phase energy change, ΔEint represents the change in internal energy, ΔEele for the electrostatic force, ΔEvdw is the change in van der Waals forces, ΔGsol, the solvation free energy, while ΔGsurf represents the non-polar contribution to the solvation-accessible surface area.

2.6. Final hits

The natural product drug molecules with cumulative inhibitory potentials for mitigating the SARS-CoV-2 infection through the viral S-protein, and with good flexibility, thermodynamic stability and strong binding affinity compared to the positive inhibitors were selected as final hits.

3. Results

3.1. Ligand preparation and Analysis of receptor active cavity

A total number of 6834 prepared minimized conformers were regenerated and saved in a 'ready-to-dock' ligprep.out file. The results of the template-free machine learning for the prediction of the active ligand binding site residues and the information from relevant literature were used to generate the x, y and z coordinates of the active pocket as 215.31, 229.77 and 282.72 respectively with a pocket score of 18.5962. This was also based on the clustered chemical neighbourhood ligandability and solvent accessible surface areas of the amino acid residues. According to relevant previous studies, the RNA-binding domain (RBD) of SARS-CoV-2 S-protein contains amino acid residues between Arg 319 - Phe 541 within its active binding pocket for S-mediated viral entry. Among the most prominently reported at the hydrophobic cleft of the receptor subunit sites are Arg 403, Asp 405, Tyr 495, Phe 497, Gln 498, Asn 501 and Tyr 505 (Lan et al., 2020; Padilla-Sanchez, 2020; Unni et al., 2020). The description of protein residue environment, accessible surface areas and interactions with estimated protonation strength of ionizable protein residue groups in terms of pKa are represented by Fig. 1. It reveals quantitative biological functions such as catalysis, molecular interactions and transportation of the amino acid groups on a structural basis. Since biological functions of enzymes are pH-dependent, the pKa values of the ionizable amino acid groups in the receptor targets are averagely between 4-11, indicating weak acids, weak bases and neutrality. These ideally support their availability for the formation of zwitterions and various molecular interactions within relevant biological environments (Jendele et al., 2019; Tan et al., 2013).

3.2. Protein preparation and receptor grid generation

The docking grid box of the minimized receptor was produced in a grid zip file. The 3D surfaces of the active pockets with docked drug molecules are presented in Fig. 2.

3.3. Molecular docking

The potentials of the natural products drug molecules to mitigate the interactions of the SARS-CoV-2 S-protein with the human ACE2 through the inhibition of the viral S-protein RBD was evaluated relatively to remdesivir and ribavirin. The binding affinities are represented by the XP glide scores and glide energy (Table 1). The five top-ranked drugs with the highest XP glide scores and good binding interactions compared to the references

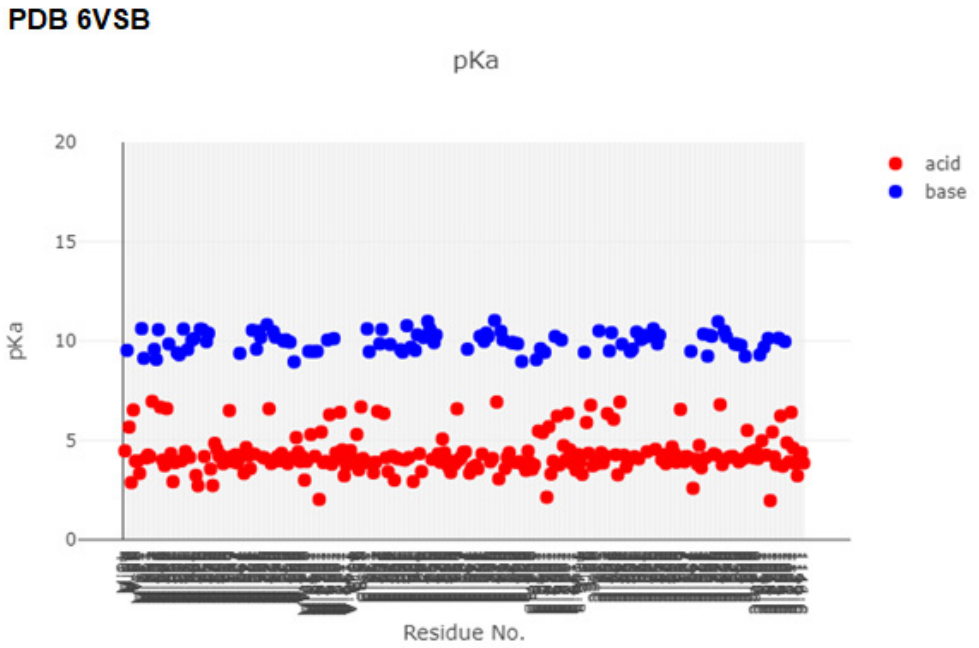

Figure 1: Prediction of pKa for ionizable Asp, Glu, Lys and His residues within binding sites of PDB 6VSB. The red and blue dots represent the positions of acids and bases respectively. The pKa values averagely fall between 4-11, indicating weak acids, weak bases and neutrality, ideal for biological systems.

are selected for analysis. They are: lonafarnib (1), (-)- epicatechin gallate (2), melibiose (3), lactitol monohydrate (4) and maltitol (5) while remdesivir (R1) and ribavirin (R2) are the references. From the results, drug 1 displayed the highest potential followed by 2, and the least affinity was observed with 5. However, all the five selected drugs showed higher binding affinities of -12.17, -11.67, -11.66, -11.30 and -10.74 kcal/mol respectively than the references R1 and R2 with -9.10 and -6.05 kcal/mol respectively, indicating stronger inhibitory potentials. From the binding poses (Fig. 3), it could be observed that the selected natural drug molecules occupied almost similar cavity volume of the receptor binding sub-pocket with the references. They mostly showed a higher number of H-bond interactions and this favours stronger binding interactions. According to the report by Lan and co-workers, the amino acid residues between Arg 319 and Phe 541 constitute the conserved RBD pocket of SARS-CoV-2 S-protein (Lan et al., 2020). All the five selected natural products drug molecules show strong hydrophilic interactions with pharmacologically essential amino acid residues within the range, consistently with remdesivir. The analysis of these interactions is essential for their promising druggability and inhibitory action against the target (Klebe, 2013). For instance, the reference drug, remdesivir displayed H-bond interactions with Tyr 369, Asn 370, Arg 403, Asp 405 and Tyr 508. Similar hydrophilic interactions were observed with the best-docked molecule 1 with Asn 370, Ser 371, Ala 372, Phe 377, Arg 403, Asp 405 and Tyr 508. Molecule 2 additionally interacted strongly with Gln 498 and Asn 501, important amino acid residues for the SARS-CoV-2 S-protein interaction with ACE2 at the N-terminal of the α1 helix, indicating a promising higher inhibitory potential against the viral entry into host (Prajapat et al., 2020). Other selected drugs also exhibited similar effects against the receptor relative to remdesivir. These infer potentials for similar but stronger inhibitory effects than the reference inhibitors (Padilla-Sanchez, 2020). The selected drugs interacted more potently with the active amino acid residues along chain A of the active RBD pocket of the receptor. This also supports their promising potentials to inhibit the viral S-protein specifically through the transmembrane protease serine 2 (TMPRSS2) cone and prevent SARS-CoV-2 cell entry (Prajapat et al., 2020).

3.4. Molecular dynamics simulation

Molecular dynamics simulation has become an essential biophysical and computational tool for studying biochemical ligand-receptor interactions (Lynch et

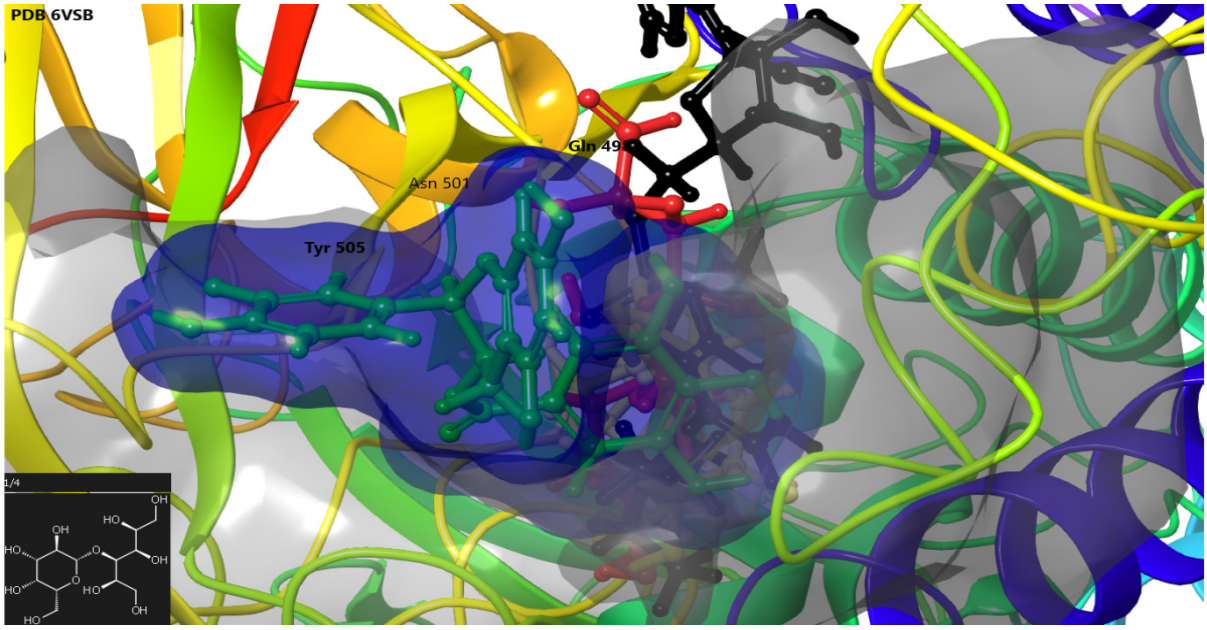

Figure 2: Surface structures of the selected drugs buried within the active RBS sites of the SARS-CoV-2 S-protein target (PDB 6VSB). The drug molecules are represented in ball and stick models: 2 (green), 3 (red), 4 (yellow) and R1 (black). The selected drugs are buried within the active RBD sub-site cavity of the receptor in stronger terms than the reference inhibitor, inferring better inhibitory interactions, especially drug 2.

Table 1: Docking results and binding free energy of selected drugs with viral S-protein (PDB 6VSB)

Drug	**Docking scores**		Molecular dynamics energy components						
	XP gscore (kcal/mol)	Glide energy (kcal/mol)	EE	VW	GE	GBS	GBT	TS	MMGB(SA) (kcal/mol)
1	-12.17	-61.25	-10.59	-45.53	-56.12	17.66	-38.46	19.98	-18.48
2	-11.67	-53.05	-6.82	-80.16	-86.98	19.45	-67.52	19.39	-48.13
3	-11.66	-66.16	-6.81	-65.76	-72.57	22.47	-50.10	20.09	-30.01
4	-11.30	-60.16	-17.39	-68.39	-85.78	31.49	-54.29	17.02	-37.27
5	-10.74	-52.90	-13.42	-43.91	-57.33	22.80	-34.52	19.21	-15.31
R1	-9.10	-43.38	-8.08	-40.48	-48.56	14.37	-34.19	14.45	-19.74
R2	-6.05	-57.95	-15.21	-47.20	-62.42	25.81	-36.61	19.17	-17.44

XP = Extra Precision; EE = Electrostatic energy; VW = van der Waals contribution; GE = total gas-phase energy; GBS = GB contribution to solvation; GBT = GB total; MMGB(SA) = final binding free energy. The table is arranged in increasing order of the XP docking scores.

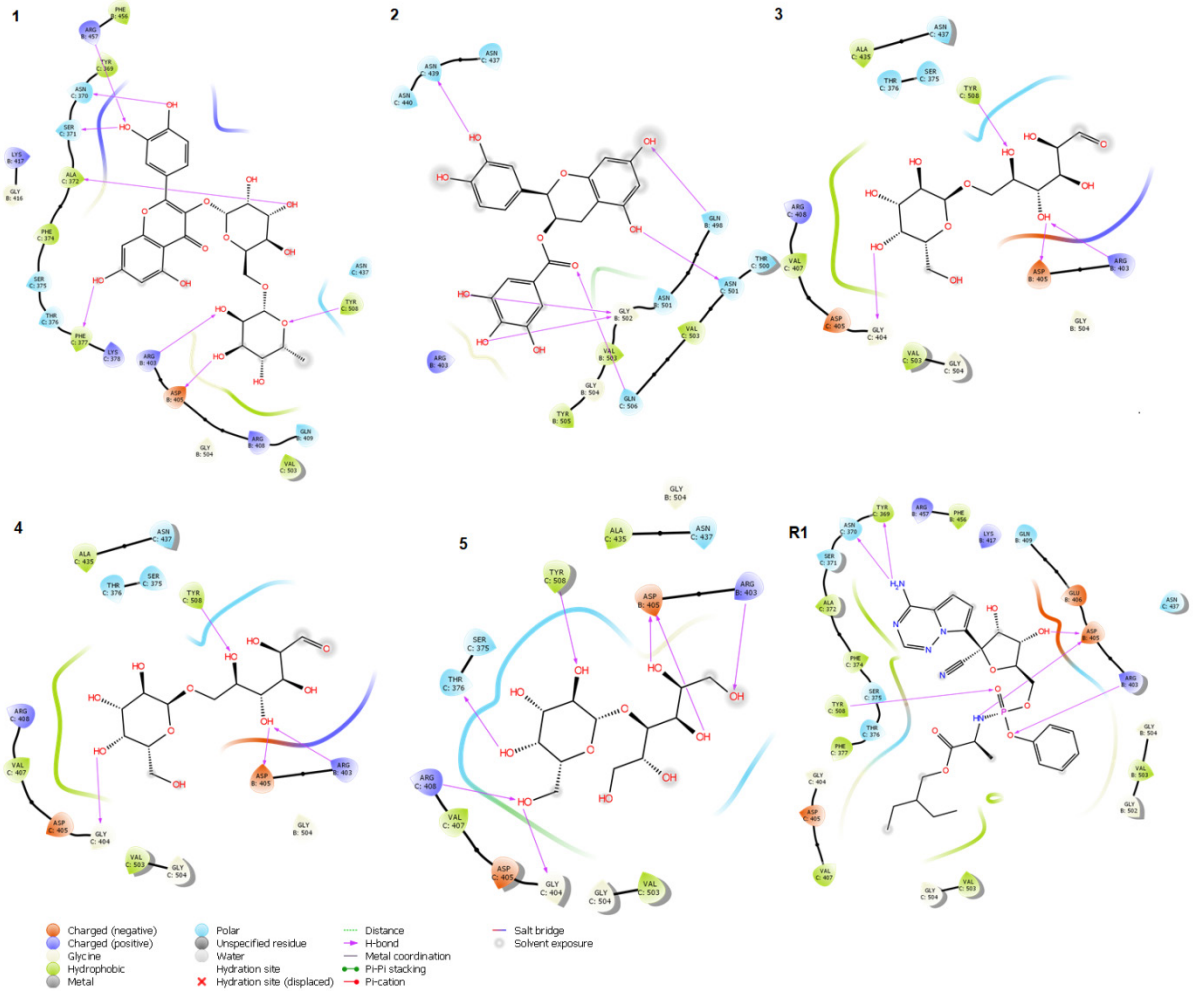

Figure 3: Binding poses of the selected drugs against PDB: 6VSB showing interactions of the selected drugs and the references with amino acid residues in the active cavity of RBD SARS-CoV-2 S-protein. Hydrogen bonding (magenta arrow), π - cation (blue line), salt bridge (red line) and π - π stacking (green line).

al., 2017). The total binding free energy, MMGB(SA) (Table 1) is a sum of GBT and TS which quantifies the existing interactions between the small flexible drug molecules and the larger bioreceptor through various conformations. Higher negative value indicates stronger binding affinity and this favours the selected drugs over the references, especially 2, 3 and 4. The statistics of H-bond (Fig. 4A) shows that drugs 4, 2, 5 and 3 experienced a higher number of hydrogen bond contacts with the amino acid residues in the receptor than the two references along the trajectories of simulation. This contributes to their higher binding free energies, consistently with the binding affinities represented by the XP scores. The higher binding affinities and binding energies ideal support stronger inhibitory potentials.

The RMSD plot (Fig. 4B) indicates that the receptor backbone initially experienced slight residue atomic deviation (2.0 - 3.5Å) at the beginning of the simulation. It became stable around 1500 ps and equilibrated with an insignificant deviation (<1.0Å) till the end of the simulation. Molecules 1-5, and the references R1 and R2, demonstrate a good stability almost throughout the simulation with insignificant deviations. This supports their compatibility to form stable complexes with the receptor. The thermodynamic motion paths, mean square isotropic displacements and transient channels which propel the ligands to enter the internal active binding cavities of the receptor are shown by RMSF plots (Fig. 4C). It could be observed that the highly unstable amino acid residues are mostly between numbers 798 – 1036, which are outside the active binding pockets. However, few of them are within the active binding pocket and as such could affect the biocompatibility with the ligands. The reference drug R1 displayed good stability with the amino acids indicated by the least fluctuation as well as drug molecules 2 and 5. These infer a good conformational stability in their drug-receptor systems along the paths of simulation. The compactness of the drug-receptor complex systems was observed to further probe the structural stability represented by the radius of rGyr plot (Fig. 4D). The rGyr is determined by the folding state of proteins in complex systems with ligands along the simulation paths. All the selected drug molecules as well as the references demonstrated a good compactness, ideal of lead-like candidates. The native contact (Q) plot (Fig. 4E) captures the transition states that exist between the drug molecules and the receptor with a folding free energy barrier to further reveal thermostability. A system consisting of an unfolding protein is indicated by a large change in Q (X) (Ayipo et al., 2021; Yang et al., 2019). Thus, the selected drug molecules display better contact with the receptor in folding states along the trajectories of simulation than the references. This also supports the stability of the receptor induced by the flexibility of the selected drug molecules. Cumulatively, drugs 1-5 show stronger inhibitory interactions with the RBD of SARS-CoV-2 S-protein than references R1 and R2. Their potentials for stability and biological functionalities are consistently better with the target compared to R1 and R2, standard inhibitors in clinical trials of COVID-19.

3.5. Final Hits

The natural drug molecules with consistent inhibitory potentials for mitigating the S-mediated SARS-CoV-2 entry into the human ACE2, and with good flexibility, thermodynamic stability and strong binding affinity compared to the positive inhibitors were selected as final hits. The selected drug molecules are currently in various stages of clinical and biomedical applications against several ailments. The results obtained in this study interestingly highlights them as potential repurposable candidates against the COVID-19 pandemic. Their pharmacokinetics, pharmacodynamics and toxicological profiles are well known (PUBCHEM, (Kim et al., 2021)), supporting their applicability for advanced experiments including preclinical and clinical trials. They are mostly present in measurable amounts in vast natural product sources except 1 which represents a synthetic analogue with ease of accessibility (Fig. 5). Impressively, some recently reported experimental studies specifically confirm drug 1 as a strong inhibitor of SARS-CoV-2 cytopathicity and RNA-dependent RNA polymerase (RdRp) (Ellinger et al., 2021; Watashi, 2020), while drug 2 was proven as a potent inhibitor of chemokine-like protease (CLpro) of SARS-CoV-2 (Du et al., 2021). Although, these are different pharmacological pathways, however, the possibilities of multi-target/network inhibitory mechanisms, commonly to natural products cannot be overruled (Joshi et al., 2020; Mansour et al., 2020; Ayipo et al., 2022), supporting the preliminary theoretical findings in this study.

4.Conclusion and recommendation

Computational molecular docking and molecular dynamics simulations have been employed to screen natural product drugs from the Selleckem.com drug repurposing library to identify potent inhibitors of the RBD of SARS-CoV-2 S-protein-mediated viral interplay with ACE2 during infection. Five drug molecules: lonafarnib, (-)-epicatechin gallate, melibiose, lactitol

Figure 4: Molecular dynamics simulation results for the selected drugs-RBD S-protein (PDB 6VSB) complexes: Hydrogen bond formation along the simulations of the selected drugs and the references with receptor within the period of 3000 ps. Stronger interactions are favoured by higher degrees of H-bond formation (A); RMSD plot of the nine selected drugs, the references and receptor backbone. The lower the deviations from the mean point the more stable the system (B); RMSF plot of the nine selected drugs. Lower fluctuations similarly infer higher stability (C); Plots of radius of gyration each ligand-receptor system. Lower differences indicate a compact and stable ligand-receptor system (D); Native of contact of the ligand-receptor system. The larger the changes in Q, the more the rigidity of the receptor which is unfavourable for a biological target (E). Thus, the analysis favour bio-functionality of the receptor and good stabilities with the selected drugs

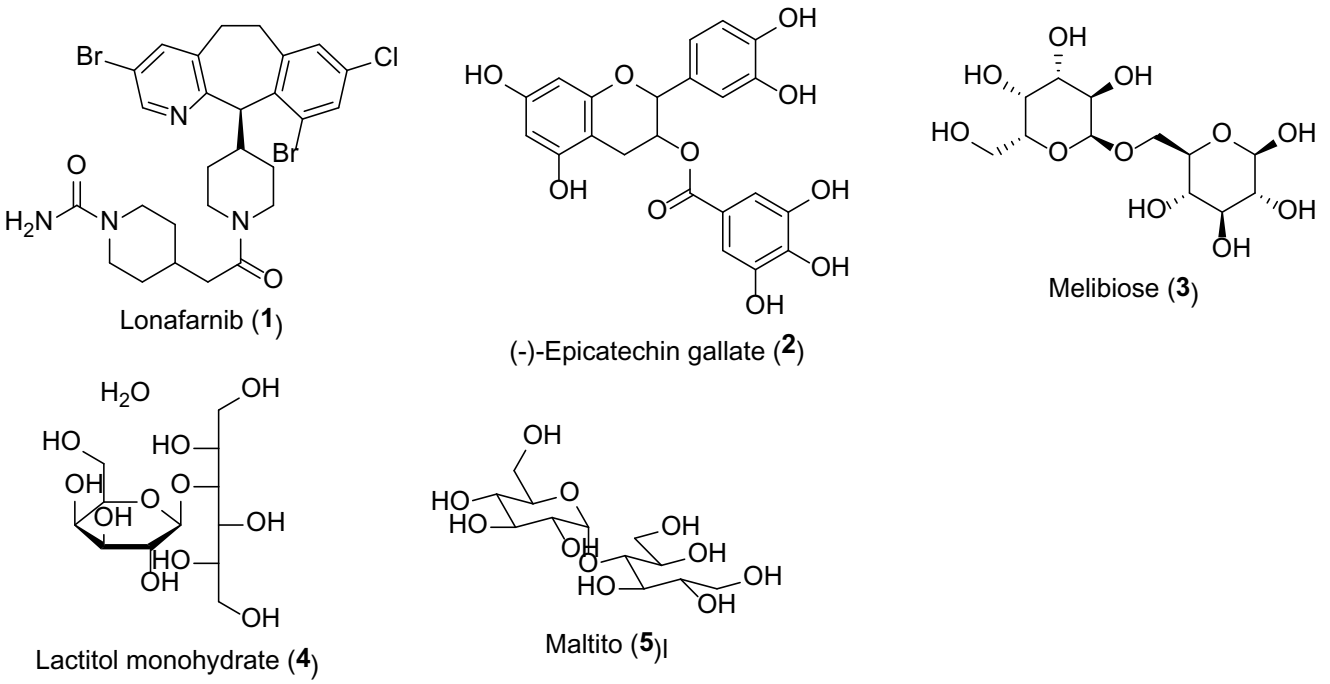

Figure 5: Chemical structure of selected potent repurposable inhibitors of SARS-CoV-2 S-protein

monohydrate and maltitol from the Selleckem.com drug repurposing library annotatively, S2797, S3925, S4758, S5282 and S3950 respectively demonstrated stronger inhibitory potentials than remdesivir and ribavirin. They displayed strong hydrophilic interactions with amino acid residues at the active RBD pocket of the receptor, potentiating ability to interrupt the interactions between the S-protein and ACE2 for SARS-CoV-2 infectivity. They showed interesting flexibility and thermodynamic stability in complex with the receptor, ideal of small-molecule prodrugs. Although, experimental investigations are required for further study through basic or clinical in vitro and in vivo models to confirm their bona fide candidacy as inhibitors of RBD SARS-CoV-2 S-protein. However, the confidence to embark on such rigorous and resource-demanding scientific exploration is hereby enhanced. The computational study represents a model for a cost-effective, faster and environmentally friendly approach towards identifying potent natural small-molecule inhibitors of SARS-CoV-2 infection for further translational studies.

References

Atri, D., Siddiqi, H. K., Lang, J., & Nauffal, V. (2020) COVID-19 for the Cardiologist: A Current Review of the Virology, Clinical Epidemiology, Cardiac and Other Clinical Manifestations and Potential Therapeutic Strategies. JACC: Basic to Translational Science. https://doi.org/10.1016/j.jacbts.2020.04.002

Ayipo, Y. O., Yahaya, S. N., Alananzeh, W. A., Babamale, H. F., & Mordi, M. N. (2021) Pathomechanisms, therapeutic targets and potent inhibitors of some beta-coronaviruses from bench-to-bedside. Infection, Genetics and Evolution, 126915. https://doi.org/10.1016/j.meegid.2021.104944

Ayipo, Y. O., Yahaya, S. N., Babamale, H. F., Ahmad, I., Patel, H., & Mordi, M. N. (2021) β-Carboline alkaloids induce structural plasticity and inhibition of SARS-CoV-2 nsp3 macrodomain more potently than remdesivir metabolite GS-441524: Computational approach. Turkish Journal of Biology. https://doi.org/10.3906/biy-2106-64

Ayipo, Y. O., Ahmad, I., Najib, Y. S., Sheu, S. K., Patel, H., & Mordi, M. N. (2022) Molecular modelling and structure-activity relationship of a natural derivative of o-hydroxybenzoate as a potent inhibitor of dual NSP3 and NSP12 of SARS-CoV-2: In silico study. Journal of Biomolecular Structure and Dynamics. https://doi.org/10.1080/07391102.2022.2026818

Bojadzic, D., Alcazar, O., Chen, J., Chuang, S. T., Condor Capcha, J. M., Shehadeh, L. A., & Buchwald, P. (2021) Small-Molecule Inhibitors of the Coronavirus Spike: ACE2 Protein-Protein Interaction as Blockers of Viral Attachment and Entry for SARS-CoV-2. ACS Infectious Diseases, 7(6), 1519–1534. https://doi.org/10.1021/acsinfecdis.1c00070

Choudhary, S., Malik, Y. S., & Tomar, S. (2020) Identification of SARS-CoV-2 Cell Entry Inhibitors by Drug Repurposing Using in silico Structure-Based Virtual

Screening Approach. Frontiers in Immunology, 11(July). https://doi.org/10.3389/fimmu.2020.01664

Du, A., Zheng, R., Disoma, C., Li, S., Chen, Z., Li, S., & Liu, P. (2021) Epigallocatechin-3-gallate , an active ingredient of Traditional Chinese Medicines , inhibits the 3CLpro activity of SARS-CoV-2 International Journal of Biological Macromolecules Epigallocatechin-3-gallate , an active ingredient of Traditional Chinese Med. International Journal of Biological Macromolecules, 176(February). https://doi.org/10.1016/j.ijbiomac.2021.02.012

Elfiky, A. A. (2020) Anti-HCV, nucleotide inhibitors, repurposing against COVID-19. Life Sciences, 248, 117477. https://doi.org/10.1016/j.lfs.2020.117477

Ellinger, B., Bojk, D., Zaliani, A., Cinatl, J., Claussen, C., Westhaus, S., Keminer, O., Reinshagen, J., Kuzikov, M., Wolf, M., Geisslinger, G., Gribbon, P., & Ciesek, S. (2021) A SARS-CoV-2 cytopathicity dataset generated by high-content screening of a large drug repurposing collection. Scientific Data, 2–11. https://doi.org/10.1038/s41597-021-00848-4

Fatoki, T. H., Ibrahim, O., Ogunyemi, I. O., Akinmoladun, A. C., Ugboko, H. U., & Adeseko, C. J.. (2021) Network analysis, sequence and structure dynamics of key proteins of coronavirus and human host, and molecular docking of selected phytochemicals of nine medicinal plants. Journal of Biomolecular Structure and Dynamics, 39(16), 6195-6217. https://doi.org/10.1080/07391102.2020.1794971

Halgren, T. A., Murphy, R. B., Friesner, R. A., Beard, H. S., Frye, L. L., Pollard, W. T., & Banks, J. L. (2004) Glide: A New Approach for Rapid, Accurate Docking and Scoring. 2. Enrichment Factors in Database Screening. Journal of Medicinal Chemistry, 47(7), 1750–1759. https://doi.org/10.1021/jm030644s

Hoffmann, M., Kleine-weber, H., Schroeder, S., Mu, M. A., Drosten, C., Po, S., Hoffmann, M., Kleine-weber, H., Schroeder, S., & Kru, N. (2020) SARS-CoV-2 Cell Entry Depends on ACE2 and TMPRSS2 and Is Blocked by a Clinically Proven Article SARS-CoV-2 Cell Entry Depends on ACE2 and TMPRSS2 and Is Blocked by a Clinically Proven Protease Inhibitor. Cell, 1–10. https://doi.org/10.1016/j.cell.2020.02.052

Jendele, L., Krivak, R., Skoda, P., Novotny, M., & Hoksza, D. (2019) PrankWeb : a web server for ligand binding site prediction and visualization. Nucleic Acids Research, 47(May), 345–349. https://doi.org/10.1093/nar/gkz424

Jin, Z., Du, X., Xu, Y., Deng, Y., Liu, M., Zhao, Y., Zhang, B., Li, X., Zhang, L., Peng, C., Duan, Y., Yu, J., Wang, L., Yang, K., Liu, F., Jiang, R., Yang, X., You, T., Liu, X., … Yang, H. (2020) Structure of Mpro from COVID-19 virus and discovery of its inhibitors. Nature. https://doi.org/10.1038/s41586-020-2223-y

Joshi, R. S., Jagdale, S. S., Bansode, S. B., Shankar, S. S., Tellis, M. B., Pandya, V. K., Chugh, A., Giri, A. P., & Kulkarni, M. J. (2020) Discovery of Potential Multi-Target-Directed Ligands by Targeting Host-specific SARS-CoV-2 Structurally Conserved Main Protease. Journal of Biomolecular Structure and Dynamics, 0(0), 000. https://doi.org/10.1080/07391102.2020.1760137

Karplus, M., & Petsko, G. A. (1990) Molecular dynamics simulations in biology. Nature, 347(May), 631–639. https://doi.org/10.1038/347631a0

Kesheri, M., & Sinha, R. P. (2016) Biomedical Image Analysis and Mining Techniques for Improved Health Outcomes (Issue January).

Kim, S., Chen, J., Cheng, T., Gindulyte, A., He, J., He, S., Li, Q., Shoemaker, B. A., Thiessen, P. A., Yu, B., Zaslavsky, L., Zhang, J., & Bolton, E. E. (2021) PubChem in 2021: New data content and improved web interfaces. Nucleic Acids Research, 49(D1), D1388–D1395. https://doi.org/10.1093/nar/gkaa971

Klebe, G. (2013) Protein–Ligand Interactions as the Basis for Drug Action. In Drug Design (pp. 61–88). https://doi.org/10.1007/978-3-642-17907-5

Kupferschmidt, K., & Cohen, J. (2020) Race to find COVID-19 treatments accelerates: WHO launches megatrial to test repurposed drugs and experimental drug candidates. Science, 367(6485), 1412–1413. https://doi.org/10.1126/science.367.6485.1412

Kumar, N., Sood, D., van der Spek, P. J., Sharma, H. S., & Chandra, R. (2020). Molecular binding mechanisms and pharmacology comparative analysis of nascapine for repurposing against SARS-CoV-2 protease. Journal of Proteome Research, 19(11), 4678-4689. https://doi.org/10.1021/acs.jproteome.0c00367

Lan, J., Ge, J., Yu, J., Shan, S., Zhou, H., Fan, S., Zhang, Q., Shi, X., Wang, Q., Zhang, L., & Wang, X. (2020) Structure of the SARS-CoV-2 spike receptor-binding domain bound to the ACE2 receptor. Nature, 581(7807), 215–220. https://doi.org/10.1038/s41586-020-2180-5

Lee, A. C. L., Harris, J. L., Khanna, K. K., & Hong, J. H. (2019) A comprehensive review on current advances in peptide drug development and design. International Journal of Molecular Sciences, 20(10), 1–21. https://doi.org/10.3390/ijms20102383

Lung, J., Lin, Y., Yang, Y., Chou, Y., Shu, Y., Cheng, Y., Liu, Y., & Wu, C. (2020) The potential chemical structure of anti-SARS-CoV-2 RNA-dependent RNA polymerase. JMV, 0–1. https://doi.org/10.1002/jmv.25761

Lynch, D. L., Hurst, D. P., Shore, D. M., Pitman, M. C., & Reggio, P. H. (2017) Molecular Dynamics Methodologies for Probing Cannabinoid Ligand / Receptor Interaction. In Cannabinoids and Their Receptors (1st ed., Vol. 593). Elsevier Inc. https://doi.org/10.1016/bs.mie.2017.05.004

Mansour, M. A., Aboulmagd, A. M., & Abdel-rahman, H. M. (2020) Quinazoline-Schi ff base conjugates : in silico study and ADMET predictions as multi-target inhibitors

of. RSC Advances, 10, 34033–34045. https://doi.org/10.1039/d0ra06424f

Musarrat, F., Chouljenko, V., Dahal, A., Nabi, R., Chouljenko, T., Jois, S. D., & Kousoulas, K. G. (2020) The anti-HIV drug nelfinavir mesylate (Viracept) is a potent inhibitor of cell fusion caused by the SARSCoV-2 spike (S) glycoprotein warranting further evaluation as an antiviral against COVID-19 infections. Journal of Medical Virology, 92(10), 2087–2095. https://doi.org/10.1002/jmv.25985

Padilla-Sanchez, V. (2020) In silico analysis of SARS-CoV-2 spike glycoprotein and insights into antibody binding. Research Ideas and Outcomes, 6. https://doi.org/10.3897/rio.6.e55281

Pervez, S. A., Karim, A., Hasan, M., Jaman, J., Karim, Z., Tahsin, T., Hasan, N,. & Hosen, M. J.. (2020). Prediction of potential inhibitors for RNA-dependent RNA polymerase of SARS-CoV-2 using comprhensive drug repurposing and molecular docking approach. International Journal of Biological Macromolecules, 163,(9), 1787-1797. https://doi.org/10.1016/j.ijbiomac.2020.09.098

Prajapat, M., Shekhar, N., Sarma, P., Avti, P., Singh, S., Kaur, H., Bhattacharyya, A., & Kumar, S. (2020) Virtual screening and molecular dynamics study of approved drugs as inhibitors of spike protein S1 domain and ACE2 interaction in SARS-CoV-2. Journal of Molecular Graphics and Modelling, 101, 107716. https://doi.org/10.1016/j.jmgm.2020.107716

Robson, B. (2020) Computers and viral diseases. Preliminary bioinformatics studies on the design of a synthetic vaccine and a preventative peptidomimetic antagonist against the SARS-CoV-2 (2019-nCoV, COVID-19) coronavirus. Computers in Biology and Medicine, 119(February), 103670. https://doi.org/10.1016/j.compbiomed.2020.103670

Tan, K. P., Nguyen, T. B., Patel, S., & Varadarajan, R. (2013) Depth : a web server to compute depth , cavity sizes , detect potential small-molecule ligand-binding cavities and predict the pK a of ionizable residues in proteins. Nucleic Acids Research, 41(June), 314–321. https://doi.org/10.1093/nar/gkt503

Ton, A., Gentile, F., Hsing, M., Ban, F., & Cherkasov, A. (2020) Rapid Identification of Potential Inhibitors of SARS-CoV-2 Main Protease by Deep Docking of 1.3 Billion Compounds. Molecular Informatics. https://doi.org/10.1002/minf.202000028

Unni, S., Aouti, S., Thiyagarajan, S., & Padmanabhan, B. (2020) Identification of a repurposed drug as an inhibitor of Spike protein of human coronavirus SARS-CoV-2 by computational methods. Journal of Biosciences, 45(1). https://doi.org/10.1007/s12038-020-00102-w

Watashi, K. (2020) Biochemical and Biophysical Research Communications Identifying and repurposing antiviral drugs against severe acute respiratory syndrome coronavirus 2 with in silico and in vitro approaches. Biochemical and Biophysical Research Communications, xxxx. https://doi.org/10.1016/j.bbrc.2020.10.094

Woldometer.info. (2021) Woldometer coronavirus. Dover, Delaware, USA.

Wu, C., Liu, Y., Yang, Y., Zhang, P., Zhong, W., Wang, Y., Wang, Q., Xu, Y., Li, M., Li, X., Zheng, M., Chen, L., & Li, H. (2020) Analysis of therapeutic targets for SARS-CoV-2 and discovery of potential drugs by computational methods. Acta Pharmaceutica Sinica B. https://doi.org/10.1016/j.apsb.2020.02.008

Xiang, R., Yu, Z., Wang, Y., Wang, L., Huo, S., Li, Y., Liang, R., Hao, Q., Ying, T., Gao, Y., Yu, F., & Jiang, S. (2021) Recent advances in developing small-molecule inhibitors against SARS-CoV-2. Acta Pharmaceutica Sinica B. https://doi.org/10.1016/j.apsb.2021.06.016

Yang, J., Wang, F., Chen, Y., Hao, G., & Yang, G. (2019) LARMD : integration of bioinformatic resources to profile ligand-driven protein dynamics with a case on the activation of estrogen receptor. Briefings in Bioinformatics, 00(August), 1–13. https://doi.org/10.1093/bib/bbz141

Yu, R., Chen, L., Lan, R., Shen, R., & Li, P. (2020) Computational screening of antagonists against the SARS-CoV-2 (COVID-19) coronavirus by molecular docking. International Journal of Antimicrobial Agents, 56(2), 106012. https://doi.org/10.1016/j.ijantimicag.2020.106012

Zhang, R., Wang, X., Ni, L., Di, X., Ma, B., Niu, S., Liu, C., & Reiter, R. J. (2020) COVID-19: Melatonin as a potential adjuvant treatment. Life Sciences, 250(February), 117583. https://doi.org/10.1016/j.lfs.2020.117583

Zhang, Z., Wu, W., Hou, J., Zhang, L., Li, F., Gao, L., Wu, X., Shi, J., Zhang, R., Long, H., Lei, M., Guo, D., Chen, K., Hofmann, L. A., & Ci, Z. (2020) Active constituents and mechanisms of Respiratory Detox Shot , a traditional Chinese medicine prescription , for COVID-19 control and prevention : network-molecular docking-LC-MS E analysis. Journal of Integrative Medicine. https://doi.org/10.1016/j.joim.2020.03.004

Zhou, Y. W., Xie, Y., Tang, L. S., Pu, D., Zhu, Y. J., Liu, J. Y., & Ma, X. L. (2021) Therapeutic targets and interventional strategies in COVID-19: mechanisms and clinical studies. Signal Transduction and Targeted Therapy, 6(1). https://doi.org/10.1038/s41392-021-00733-xFarouque, G., &, Takeya, H. (2007) Farmers' perception of integrated soil fertility and nutrient management for sustainable crop production: a study of rural areas in Bangladesh, *Journal of Agricultural Education*, *48*(30), 111 – 122. DOI: 10.5032/jae.2007.03111